# Atomistic model of reptation at polymer interfaces*

D.G. Luchinsky*† H. Hafiychuk†, M. Barabash* V. Hafiychuk†, T. Ozawa‡ and K. R. Wheeler§, P.V.E. McClintock*
*Department of Physics Lancaster University, Lancaster, UK, LA1 4YB
Email: d.luchinsky@lancaster.ac.uk
†SGT Inc., ARC, Moffett Field, California, 94035, USA
‡Materials Science Section, Engineering Technology Division, JSOL Corporation, JP
§ARC, Moffett Field, California, 94035, USA

Abstract—We study a molecular dynamics model of a polymer-polymer interface for a polyetherimide/polycarbonate blend, including its thermodynamic properties, its chain reptation, and its corresponding welding characteristics. The strength of the sample is analyzed by measuring strain-stress curves in simulations of uni-axial elongation. The work is motivated by potential applications to 3D manufacturing in space.

Index Terms—polymer interfaces, reptation, welding, strength of the interface

## I. Introduction

Understanding the properties of polymer-polymer interfaces is a long-standing problem of fundamental and technological importance [1]. In particular, basic properties such as reptation and entanglement determine the welding dynamics and strength in fused deposition modeling [2]. The atomistic structure of polymers substantially influences these properties. However, earlier research was mostly focused either on bulk properties [3] or on coarse-grained models of interfaces [4].

Here we report the development and analysis of a fully atomistic model of a polymer-polymer interface in a blend of polyetherimide (PEI) polycarbonate (PC) representing material ULTEM 9085, which us currently widely used in aerospace applications. We use molecular dynamics (MD) simulations to investigate the diffusion of polymer chains at the interface and thus estimate the initial time scales for reptation and welding. We assess the thermal and mechanical properties of the blend in the presence of a planar interface and characterise the strength of the interface as a function of the welding time, using strain-stress measurements in uni-axial elongation simulations.

The paper is organized as follows. First, we introduce the model and discuss its validation in Sec. II. Next, in Sec. III, we analyse the diffusion of chains at the interface. The strength of the interface as a function of welding time is discussed in Sec. IV. Finally, conclusions are drawn and presented in Sec. V.

## II. Model

We investigate blend composition consisting of 80% PEI and 20% PC, which corresponds to the optimal miscibility of these polymers and is commonly used in ULTEM 9085. Amorphous cells of these blends were prepared and relaxed at temperature $T_0 = 600$ K (or 650K) using the software package J-OCTA [5] and the following procedure: (i) equilibration in the microcanonical (NVE) ensemble; (ii) compression in the isothermal–isobaric (NPT) ensemble to a pressure $P = 100$ MPa; (iii) additional NVE equilibration; (iv) relaxation in the NPT thermostat; and (v) elimination of the translational velocity in the canonical (NVT) Andersen thermostat. Each step was computed during 100 ps with a time step of 1 fs. The simulations used software from LAMMPS [6] and GROMACS [7] as well as from J-OCTA [5].

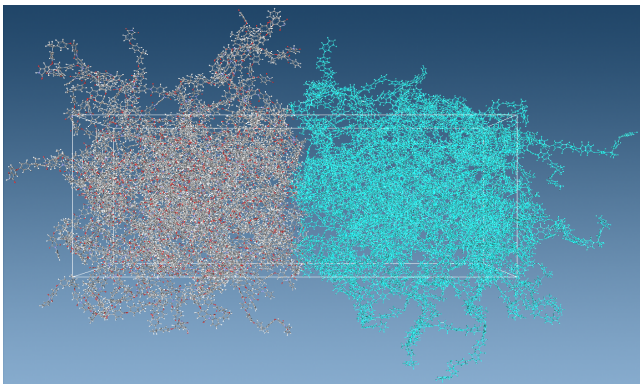

Fig. 1. Two amorphous cells (grey and cyan) of PEI/PC polymer blend are combined in one chemical sample across an atomically flat interface.

A nearly atomically flat boundary on each cell was prepared using the Lennard-Jones potential, and the cells were then brought together across this almost flat interface as shown in Fig. 1. The total size of the sample was 41328 atoms, 96 PEI chains and 48 PC chains, with 5 repeating units in each chain. The welding process was simulated during 240 ns at $T_0 = 600$ K and $P_0 = 1$ bar. Fast quenching to 300 K was performed after 60 ns and 240 ns, in 12 steps of 25K and 2 ns, each using the NPT ensemble. Additional thermal cycling between 600 K and 300 K was performed with time steps varying between 12 ns and 25 ns.

The resultant samples at different temperatures were

Leverhulme Trust Research Project Grant RPG-2017-134 and NASA STMD/GCD/LSM grant in Space Manufacturing

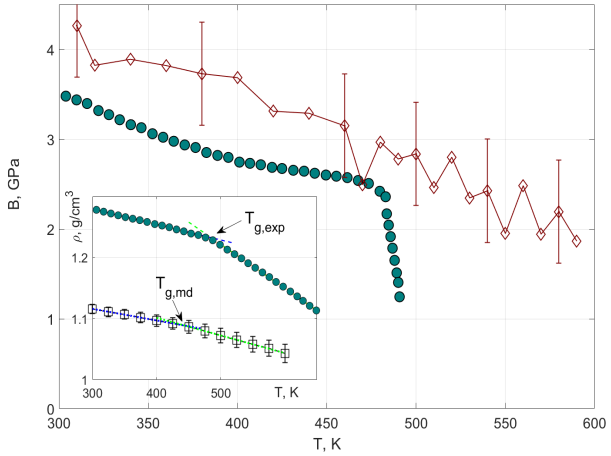


Fig. 2. $B(T)$ estimated fluctuations (red open diamonds) in comparison with experimental data obtained for ULTEM 1000 [8] (teal circles). The inset shows the temperature dependence of the density $\rho(T)$ obtained in MD calculations as compared to the experimental data obtained for ULTEM 1000 [8] (teal circles). The dashed lines show linear fit to the low (green) and high (blue) temperature regions of $\rho(T)$. The glass transition temperatures corresponding to the intersections of the straight lines are shown by arrows.

used to estimate the properties of the PEI/PC blend. The results of the simulations were compared to experimental data available online for pure polyetherimide ULTEM 1000 [8]. Here we provide two examples of such a comparison, as shown in Fig. 2, further details are available in [9]. The first example shows the results of the bulk modulus ($B$) simulations in comparison with experimental data. The MD results were obtained using the fluctuational formula $B = V\left\langle \sigma_V^2 \right\rangle / k_B T$, where $V$ is the volume, $\sigma_V^2$ is its variance, and $k_B$ is the Boltzmann constant. The experimental data for $B$ were estimated using measurements of Young's modulus $E$ and the equation $B = E/3(1-2\nu)$, taking a nominal value of Poisson's ratio $\nu = 0.36$. The comparison is only available for temperatures below the glass transition temperature $T_g \sim 475$ K. The MD results are in reasonable agreement with the experimental data.

In the second example, the density $\rho$ from the MD simulations is compared to the experimental data as a function of temperature, as shown in the inset of Fig. 2. As obtained from the MD simulations, $\rho$ is $\sim 15$ % less than in the experiments, which is within acceptable accuracy for MD predictions [10]. In addition, as shown in the figure, the intersection of the straight line sections of $\rho(T)$ below and above the glass transition allows one to estimate $T_g$. The values of $T_g$ obtained in MD and experiment are 451 K and 485 K (ULTEM 1000) respectively. Note, that the experimental value of $T_g$ provided by StratSys for ULTEM 9085 [11] is 459. K, which is closer to our estimate.

Similar results were obtained for the MD estimates of the thermal expansion coefficient [9]. Reasonable agreement with experimental data was found for temperatures below $T_g$. Above $T_g$, experimental data were not available. Overall, we can conclude that MD simulations of the PEI/PC blends provide results consistent with experimental observations. We now consider the results of the welding analysis in these samples.

## III. Interface diffusion

The diffusion at an interface is the key process that defines strength of the manufacturing parts [1]. To provide atomistic insight into diffusion dynamics we analyzed reptation in two samples. The first sample was as described in the Sec. II. The second sample was larger and had longer chains: 130 PEI chains each 6 monomer units long and 50 PC chains each 8 monomer long. The total size of this sample was 67912 atoms. The sample was equilibrated using method described in Sec. II at temperature 650 K. The reptation dynamics was qualitatively similar in both samples. Here we describe some results of the analysis performed for the larger sample.

An example of the analysis of chain reptation at the interface for this sample is shown in Fig. 3 for welding at $T = 650$ K.

The motion of the semiflexible chains on a time scale of our simulations $\sim$300 ns occurs via reptation when the chain remains within a "tube" determined by the intersections with neighboring chains, and the end of the chain moves slowly across the interface in a random fashion. A snapshot of this motion is shown in the inset of Fig. 3 after $\sim$40 ns of welding. The interface is shown by the transparent blue plane, the atomic structure of the chain is shown by thin gray lines, and the core of the chain is shown by the blue solid line. The gray dots show the locations of the chains that constrain motion of a given chain and shape its reptation "tube" within 10 Å radius of the core. The coarse-grained sub-units of the chain crossing the interface are shown by red dots. Note that initially all sub-units of this chain were on one side of the sample.

The simulations reveal a few time scales of reptation during 300 ns of welding. The first time scale of $\sim$50 ps corresponds to the so-called "wetting" process when the two surfaces quickly come close to each other [12] attracted by electrostatic and van der Waals forces. Next, we observed a fast diffusion of polymer chains on a time scale of $\sim$20 ns while the density of atoms at the interface was rising rapidly towards its bulk value. We attribute fast diffusion to the initial existence of relatively "free" chain ends and "vacancies" on the both sides of the interface. Finally, we observed a slow diffusion of the chains across the interface into the bulk of the sample on the other side, cf. [13].

The profiles of the atomic densities on the two sides of the interface, corresponding to these time scales, are shown in Fig. 3. It can be seen from the figure that the two samples are initially well separated, with the half-width of the gap at half bulk density $\sim$5Å. After $\sim$0.5 ns the density at the interface has nearly reached its bulk value. After another 40 ns the density profiles stay almost

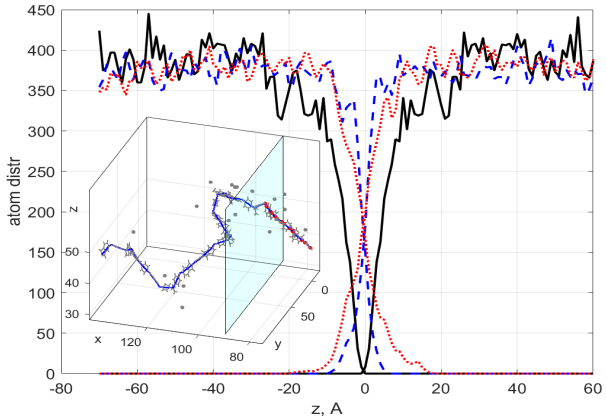


Fig. 3. Atom density profiles of the polymers on both sides of the interface: (i) initial (black solid lines); (ii) at ∼0.5 ns (blue dashed lines); (iii) at ∼40 ns (red dashed lines). The inset shows example of a single chain reptation at the interface.

the same with only the tails of the distributions extending to the other side by nearly 20 Å.

This extension of the distributions tails has a profound effect on the strength of the interface. Indeed, according to Wool [14] the full strength is obtained when the two polymers filaments are interdiffused at the distance equal to 81% of the radius of gyration ($R_g$). Note, that for PEI/PC blends the interfacial strength is mainly determined by interdiffusion of the PEI chains. The radius of gyration in $z$-direction estimated in our simulations for PEI chain was $R_{gz}$ ∼18 Å and for PC chain $R_{gz}$ ∼7.5 Å. This corresponds to the maximum extension of PEI chains ∼50 Å and for PC chains ∼25 Å.

Therefore, we expect complete healing of the interface when maximum extension of the chains in $z$-direction is ∼40 Å. We observe, however, a substantial slowing down of the tails extension beyond 20Å. This slowing down is attributed to the structure of the blend samples that has 20% of PC and 80% of PEI chains. PC chains being smaller and more flexible diffuse much faster towards the interface while it takes more time to equilibrate for stiffer and longer PEI chains.

The two different time scales for interdiffusion of PEI and PC chains were directly observed in simulations by following in time the distributions of the center of masses (CMs) of individual chains. It was found that the CMs distribution of PC chains bridges initial gap at the interface and becomes nearly uniform at the time scale of the order of 200 ns. The CMs distribution of the PEI chains tends towards equilibrium but remains nonuniform with the gap at the interface up to 300 ns.

We conclude that in our simulations the strength of the interface is approaching the bulk value as a function of time but the curing process remains incomplete. The interface strength on the time scale of simulations will be mainly determined by the interdiffusion of PC chains and will be lower than the one expected for polyetherimide.

We now provide the details of the MD estimations of the sample strength as a function of welding time.

## IV. Interface strength

To test the interface strength as a function of welding time, we performed uni-axial elongation of the samples at constant rate in the $z$-axis direction using the scenario developed by J-OCTA [5]. During deformation, the sample eventually breaks at the interface. The breaking-up process involves stretching the chains and pulling them out of the bulk of the sample. In addition, the separation process requires the "wetting" potential barrier related to the non-bonding interaction energy between the two samples to be overcome. The thinner the welded layer, the smaller is the strain at which the breakup process is expected to be observed.

The measurements of the elongation have to be performed by resolving the breaking dynamics. Here we demonstrate the results of preliminary analysis obtained for elongation rate 50 m/s with time step 0.5 fs using VSOP solver developed by J-OCTA [5].

The strain-stress curves obtained in the MD simulations for three different welding times are compared with the experimental curve in Fig. 4. The curves deviate from the experimental data due to the high elongation rate used in the MD simulations. However, it can be seen from the figure that both Young's modulus and the Yield strength increase as the thickness of welded layer increasing. We note that the calculations were performed under assumption of nominal Poisson's ratio $\nu = 0.36$. This assumption becomes increasingly inaccurate as the breaking of the sample is initiated at the interface. For this reason the strain-strees curves obtained in MD are shown by the dashed lines for the values of strain larger than 0.1.

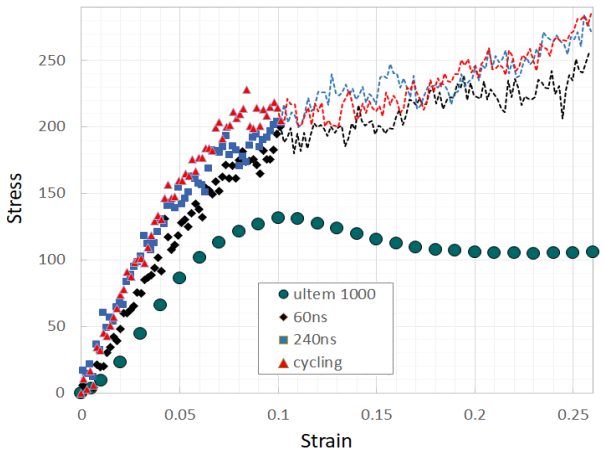


Fig. 4. MD simulations of the strain-stress curves as a function of welding time: (i) 60 ns (diamonds); (ii) 240 ns squares; and (iii) after additional welding during temperature cycling (1200 ns). The experimental data obtained by ULTEM 1000 [8] are shown by teal shaded circles.

We also note that we have not observed the expected decrease of the Yield strength (see discussion in the end of the previous section). We attribute this discrepancy to the large elongation rate used in MD simulations.

The value of the Young's modulus obtained in MD simulations

$$E \sim 2\ GPa$$

is slightly smaller than the value 2 - 2.5 GPa estimated using open data source [11]. We note, however, that the obtained value of Young's modulus is in good agreement with the data reported for ULTEM 1000 [8] shown in the figure by open teal circles.

## V. Conclusions

In summary, we have developed a fully atomistic molecular dynamics model of the polyetherimide/polycarbonate amorphous polymer blends. Two cells were brought together to form a sample with an atomically nearly flat interface and were allowed to equilibrate for 240 ns. The sample was quickly quenched to 300 K after 60 and 240 ns of welding at the interface. Additional thermal cycling between 300 and 600 K was performed after quenching at 240 ns.

The model was validated by comparison of the MD predictions with experimental data for the density, glass transition temperature, bulk modulus, and thermal expansion coefficient below $T_g$ (where experimental data were available).

The model was used to analyze diffusion of the polymer chains at the interface during the welding process and to estimate the interface strength as a function of welding time. It was shown that, after the initial "wetting" process, the diffusion take place via snakelike motion of the polymer chains. Two characteristic time scales were observed during the first 300 ns of welding: (i) fast diffusion ($t \lesssim$ 20 ns) when chain's ends can diffuse by filling in vacancies on both sides of the interface; and (ii) slow diffusion ($t \lesssim$ 300 ns) when chain's ends slowly diffuse through the bulk material on both sides of the interface.

The analysis of the strain-stress curves as a function of time reveals the effect of the thickness of the welded layer on the strength of the interface. It was shown that both Young's modulus and the Yield strength increase as the thickness of welded layer increasing. The deviations of the strain-stress curves obtained in MD simulations from the experimental data attributed to the large elongation rate and relatively large time step used in the simulations. In the future work the effect of both elongation rate and the time step will be verified.

Overall, the good agreement of the developed model with experimental data paves the way to semi-quantitative predictions of the interface properties of the polymer blends considered.


## Acknowledgments

We thank Gabriel Jost for the help in running simulations on Amazon Web Services. We are grateful to Hiroya Nitta and Kenta Chaki for support and valuable discussion. We thank Tracie Prayer for providing experimental data and guidance.


## References


[1] S. Prager and M. Tirrell, "The healing process at polymer-polymer interfaces," The Journal of Chemical Physics, vol. 75, no. 10, pp. 5194–5198, nov 1981.

[2] Q. Sun, G. Rizvi, C. Bellehumeur, and P. Gu, "Effect of processing conditions on the bonding quality of FDM polymer filaments," Rapid Prototyping Journal, vol. 14, no. 2, pp. 72–80, 2008.

[3] S. G. Falkovich, S. V. Lyulin, V. M. Nazarychev, S. V. Larin, A. A. Gurtovenko, N. V. Lukasheva, and A. V. Lyulin, "Influence of the electrostatic interactions on thermophysical properties of polyimides: Molecular-dynamics simulations," Journal of Polymer Science Part B: Polymer Physics, vol. 52, no. 9, pp. 640–646, feb 2014.

[4] T. Ge, M. O. Robbins, D. Perahia, and G. S. Grest, "Healing of polymer interfaces: Interfacial dynamics, entanglements, and strength," Phys. Rev. E, vol. 90, p. 012602, Jul 2014.

[5] User's Manual, J-OCTA Overview, J-OCTA 4.0, JSOL corp., 2018. [Online]. Available: http://www.j-octa.com/

[6] T. W. Sirk, S. Moore, and E. F. Brown, "Characteristics of thermal conductivity in classical water models," The Journal of Chemical Physics, vol. 138, no. 6, p. 064505, feb 2013.

[7] S. Páll, M. J. Abraham, C. Kutzner, B. Hess, and E. Lindahl, "Tackling exascale software challenges in molecular dynamics simulations with GROMACS," in Lecture Notes in Computer Science. Springer International Publishing, 2015, pp. 3–27.

[8] "Heat capacity," https://www.protolabs.com/media/1014801/ultem-1000-im.pdf, ULProspector.com, UL LLC., 2018.

[9] D. G. Luchinsky, H. Hafiychuk, V. Hafiychuk, and K. Wheeler, "Molecular dynamics of ultem 9085 for 3d manufacturing: spectra, thermodynamic properties, and shear viscosity." NASA, ARC, Tech. Rep. to be published NASA/TM, 2019.

[10] C. Li, G. A. Medvedev, E.-W. Lee, J. Kim, J. M. Caruthers, and A. Strachan, "Molecular dynamics simulations and experimental studies of the thermomechanical response of an epoxy thermoset polymer," Polymer, vol. 53, no. 19, pp. 4222–4230, aug 2012.

[11] "Ultem 9085 production-grade thermoplastic for fortus 3d printers," https://www.stratasys.com/-/media/files/material-spec-sheets/mss_fdm_ultem9085_1117a.pdf, MatWeb Lcc, 2019.

[12] E. Jabbari and N. A. Peppas, "Polymer-polymer interdiffusion and adhesion," Journal of Macromolecular Science, Part C: Polymer Reviews, vol. 34, no. 2, pp. 205–241, may 1994.

[13] H.-P. Hsu and K. Kremer, "Static and dynamic properties of large polymer melts in equilibrium," The Journal of Chemical Physics, vol. 144, no. 15, p. 154907, apr 2016.

[14] R. Wool, Polymer Interfaces: Structure and Strength. Hanser Publishers, 1995.